TENTH AUSTRALASIAN FLUID MECHANICS
CONFERENCE - UNIVERSITY OF MELBOURNE
11-15 DECEMBER 1989



# ON THE DEVELOPMENT OF A TURBULENT FREE TRIANGULAR JET

W.R. QUINN

Department of Engineering
St. Francis Xavier University
Antigonish, Nova Scotia B2G 1C0
CANADA

## ABSTRACT

Detailed mean flow and turbulence measurements have been made, using hot-wire anemometry, in the near flow field of a turbulent, incompressible, isothermal air jet, issuing from a sharp-edged equilateral triangular slot into stagnant air surroundings. The measured quantities include the three components of the mean velocity vector, the streamwise turbulence intensity and two of the Reynolds shear stresses. The results indicate that the jet spreads faster on its base side than at its apex. This leads to in an inversion of the jet shape at about five equivalent slot diameters downstream of the slot exit plane. The Reynolds shear stress levels, compared to those found in round turbulent free jets at the same downstream locations, are higher in the triangular jet, implying improved mixing.

## INTRODUCTION

Turbulent free triangular jets, like other turbulent free jets issuing from noncircular slots or nozzles, find use or have the potential for usage in technical areas of interest ranging from aerospace to chemical to mechanical engineering. Some areas of application of triangular jets are in combustion chambers of jet engines, boiler furnaces and gas-turbine plants of electric power utilities. Rapid mixing is a prerequisite for good performance in most applications. Economic expediency may, in some applications, require that sharp-edged slots be used in preference to nozzles with contoured upstream shaping.

Previous experimental work on turbulent free triangular jets (Gutmark et al. (1985), Schadow et al. (1988) and Koshigoe et al. (1988)) has involved jets issuing from either isosceles and equilateral triangular ducts or from isosceles and equilateral triangular orifices, with small upstream bell-mouth radii, attached to pipes of circular cross-section. These flow configurations occur, along with sharp-edged slots, in practical systems. The flow of a turbulent free jet, issuing from a sharp-edged triangular slot has thus far, however, not been studied.

This study presents detailed mean flow and turbulence data for the flow, in the near flow field, of a turbulent, incompressible, isothermal air jet, issuing from a sharp-edged equilateral triangular slot, into stagnant isothermal air surroundings. The decay of the mean streamwise velocity along the jet centreline is also presented. The slot exit plane Reynolds number, based on the equivalent diameter of the triangular slot (same as the diameter of a round slot with the same exit area as the triangular slot), was about 2.08 x $10^5$. The mean streamwise velocity and streamwise turbulence intensity at the centre of the slot exit plane were 60 m/s and 0.5% respectively.

## EXPERIMENTAL SET-UP AND PROCEDURE

The flow facility, described in detail in Quinn & Militzer (1988), is of the blow-down type and consists of a small centrifugal fan, a settling chamber, a three-dimensional contraction and the sharp-edged equilateral triangular slot.

The sensing probe is moved in the flow field by a stepping-motor-driven, microcomputer-controlled, three-dimensional traversing system. A definition sketch of the coordinate system and the corresponding components of the mean velocity vector is given in Fig. 1. A rack and pinion system is used for traversing in the X-direction and lead screws are used for traversing in the Y- and Z-directions.

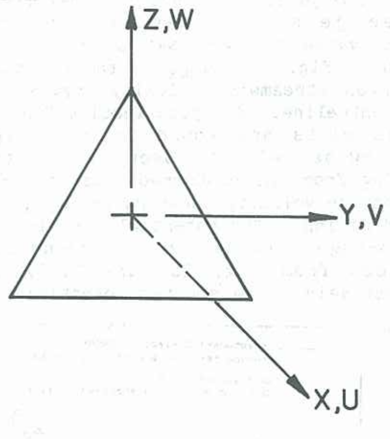


Figure 1 Definition sketch for the coordinate system

X-array hot-wire probes were used for the mean flow and turbulence measurements. The hot-wire probes, operated by linearized constant temperature anemometers at a resistance ratio of 1.8, were calibrated in the initial region of the test jet. A 12-bit A/D board, with 16 analog input channels, a multiplexer and a sample-and-hold unit, was used to digitize the hot-wire signals. Signal conditioning was effected by two other sample-and-hold units, low-pass analog filters and amplifiers. The mean and rms fluctuating velocities were obtained by sampling, depending on the location in the flow, between 75,000 and 100,000 points at 1 kHz.

RESULTS AND DISCUSSION

The decay of the mean streamwise velocity, $U_{C\ell}$, along the jet centreline is shown in Fig. 2a. The results, obtained in the same test rig as that used for the triangular jet, for jets issuing from a sharp-edged round slot and from a contoured round nozzle with the same exit area as the triangular slot, are included for comparison. $U_{exit}$ is the value of the mean streamwise velocity at the centre of the slot exit plane and $D_e$ is the equivalent diameter of the triangular slot or the diameter of the round slot. The vena contracta effect, associated with sharp-edged slots (see e.g. Daugherty et al. (1985)), is clearly evident. By contrast, the jet issuing

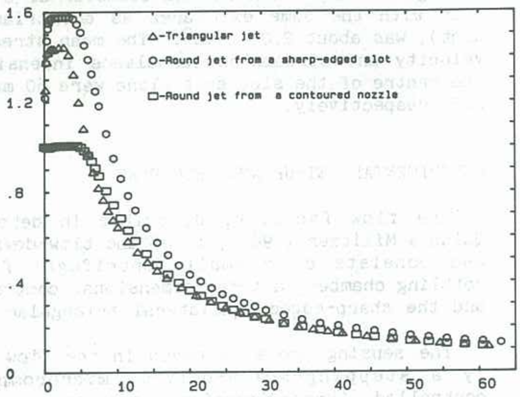


Figure 2a Mean streamwise velocity decay along the jet centreline

from the contoured nozzle does not have the exit mean streamwise velocity overshoot found in the other two jets. The inverse decay plots for the three jets and that for the round jet investigated by Wygnanski & Fiedler (1969) are shown in Fig. 2b. $U_{max}$ is the maximum value of the mean streamwise velocity anywhere along the jet centreline. The jets issuing from the sharp-edged slots are found to have higher mean streamwise velocity decay rates than those issuing from the contoured nozzles. Higher mean streamwise velocity decay rates imply better far-field mixing. The potential core lengths of the sharp-edged triangular and round slot jets, deduced from Fig. 2b, are $3.1D_e$ and $4.4D_e$ respectively. The shorter potential core length

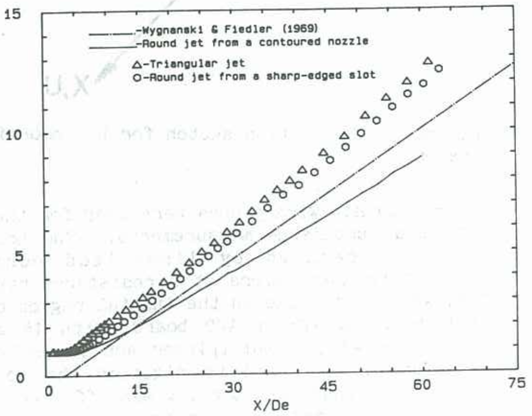


Figure 2b Inverse decay plots

of the triangular jet, also evident in Fig. 2a and in agreement with results of Gutmark et al. (1985), indicates better near-field mixing.

Mean streamwise velocity contour plots at four downstream stations are presented in Figs. 3a, 3b, 3c, & 3d. In the region close to the slot exit plane (Fig. 3a), the contours have the triangular shape prescribed by the slot.

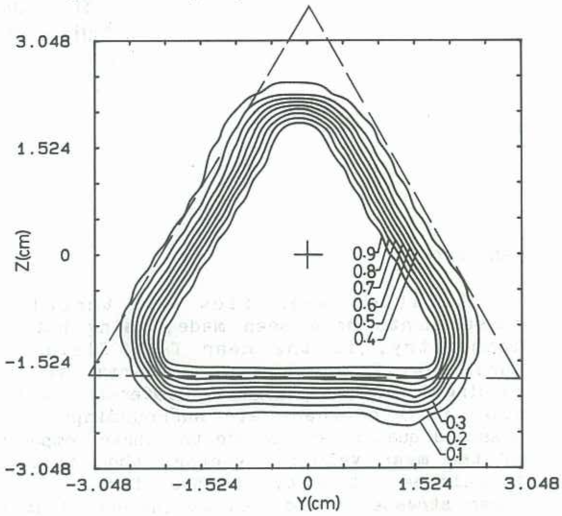


Figure 3a $U/U_{C\ell}$ contours at $X/D_e$ = 0.5

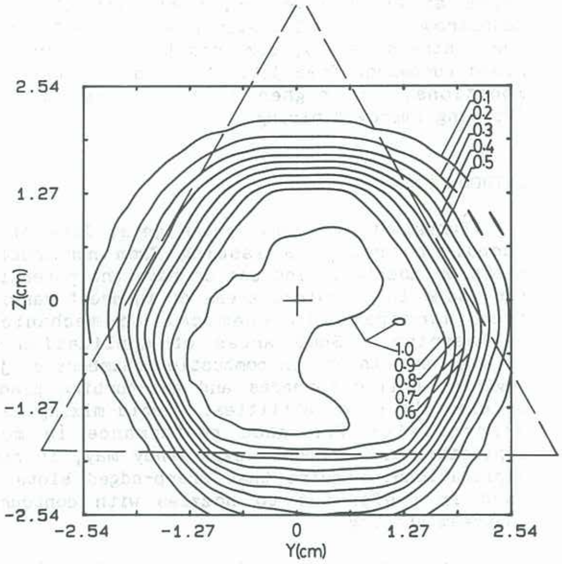


Figure 3b $U/U_{C\ell}$ contours at $X/D_e$ = 1.0

Furthermore, the 0.5 contour is further away from the centre of the jet, shown by a cross in Fig. 3a and in all subsequent figures, on the apex side than on the base side of the jet. This indicates faster spreading of the jet on its apex side in this region of the flow. At $X/D_e$ = 1 (Fig. 3b), the contours have a quasi-axisymmetric shape and spreading on the base side is now faster than on the apex side. Further downstream (Figs. 3c & 3d), the contours have an inverted triangular shape but faster spreading still occurs on the base side of the jet as viewed from the slot exit plane. The changing shape of the mean streamwise velocity of the jet as it develops downstream is, in view of the subsequent discussion in connection with the Reynolds stresses, noteworthy. The difference in the size of the triangular slot, superimposed with dashed lines on all the figures showing contour maps, is brought about by the contour-plotting software which enlarges the measurement grid for $X/D_e \leq 1$ and contracts it for $X/D_e > 1$.

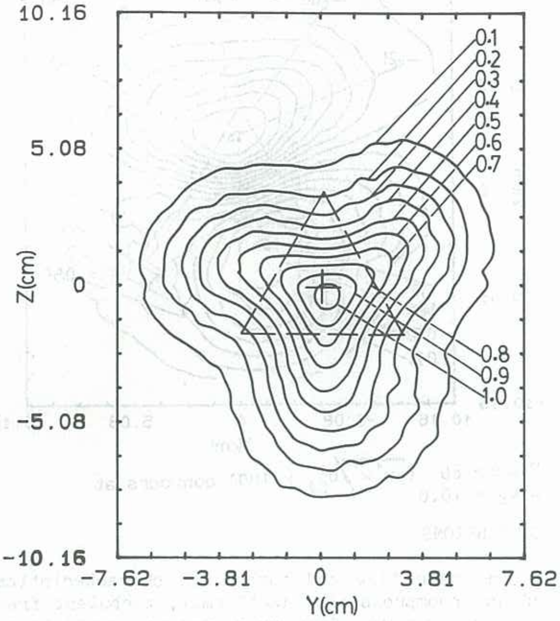


Figure 3c $U/U_{C\ell}$ contours at $X/D_e$ = 5.0

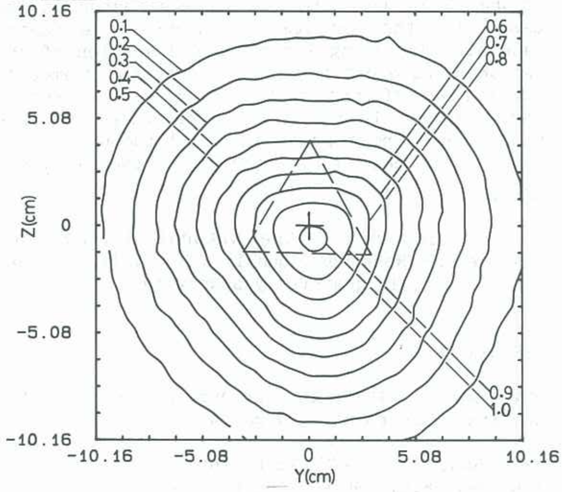


Figure 3d $U/U_{C\ell}$ contours at X/De = 10.0

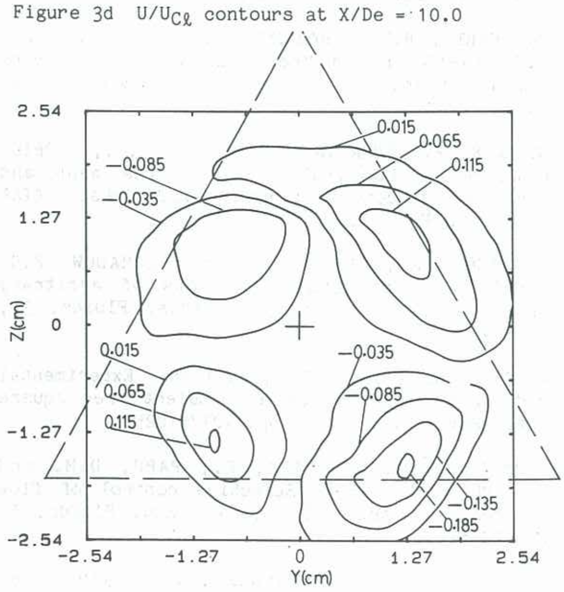


Figure 4a $V/U_{C\ell}$ contours at $X/D_e$ = 1.0

Contours of the mean spanwise velocity, V, and the mean lateral velocity, W, are shown in Figs. 4a & 4b respectively. The secondary flow pattern in the near flow field appears to be made up of four counterrotating cells. The spanwise secondary flow cells suggest flow away from the jet at the apex side and flow into the jet at the base side. The lateral secondary flow cells suggest flow from the apex side into the base side of the jet. The combined effect of the spanwise and lateral secondary flow cells is consistent with the faster spreading of the jet on its base side as noted earlier.

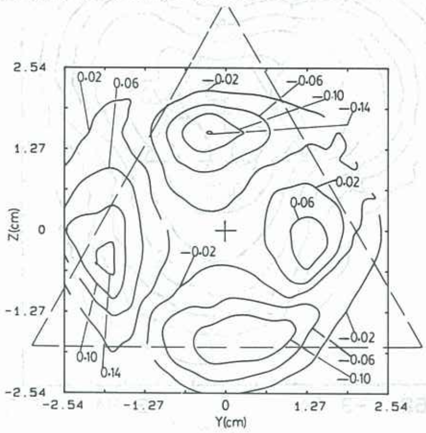


Figure 4b $W/U_{C\ell}$ contours at $X/D_e$ = 1.0

The streamwise turbulence intensity contours are presented in Figs. 5a, 5b & 5c. Spanwise and lateral turbulence intensities were also measured but contour maps for these quantities are, for space reasons, not presented here. There is a close correspondence between the shapes of the mean streamwise velocity contours presented in Figs. 3b, 3c & 3d and those of the streamwise turbulence intensity contours in Figs. 5a, 5b & 5c. Furthermore, large streamwise turbulence intensity gradients are found, as expected (see Bradshaw (1975)), in regions where the local shear is high and vice versa.

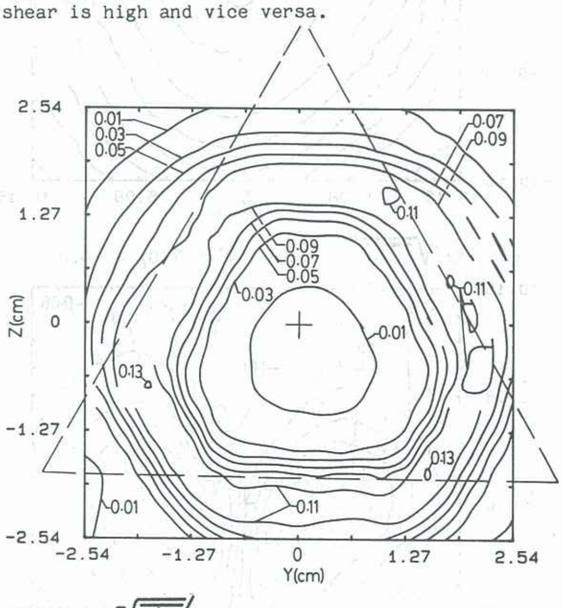


Figure 5a $\sqrt{\overline{u'^2}}/U_{C\ell}$ contours at $X/D_e$ = 1.0

The Reynolds shear stress contours are shown in Figs. 6a & 6b. Like the streamwise turbulence intensity, large Reynolds shear stress gradients are also found in regions of the flow where the local shear is high. The Reynolds stress gradients generate secondary flows of Prandtl's second kind (Bradshaw (1987)) which account for the change in the shape, noted earlier, of the mean streamwise velocity during the downstream development of the jet.

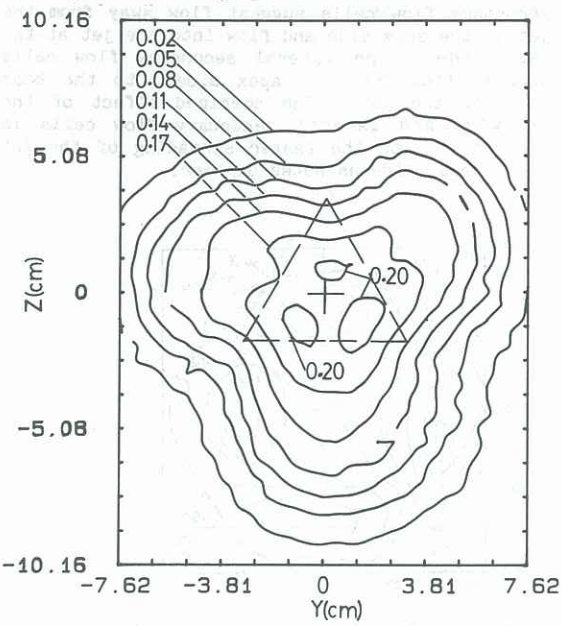


Figure 5b $\sqrt{\overline{u'^2}}/U_{C\ell}$ contours at $X/D_e$ = 5.0

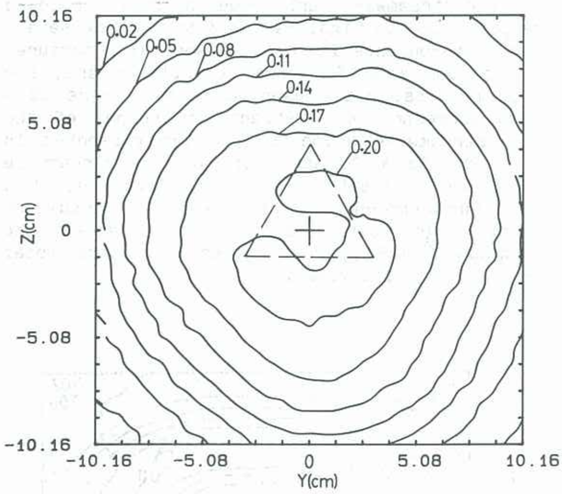


Figure 5c $\sqrt{\overline{u'^2}}/U_{C\ell}$ contours at $X/D_e$ = 10.0

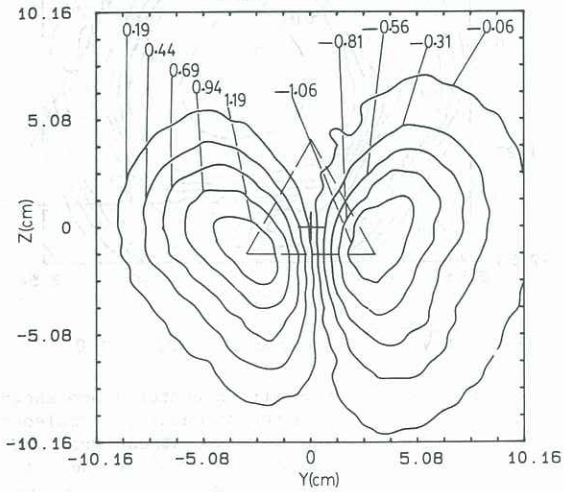


Figure 6a $(\overline{-u'v'}/U^2_{C\ell}$ x 100) contours at $X/D_e$ = 10.0

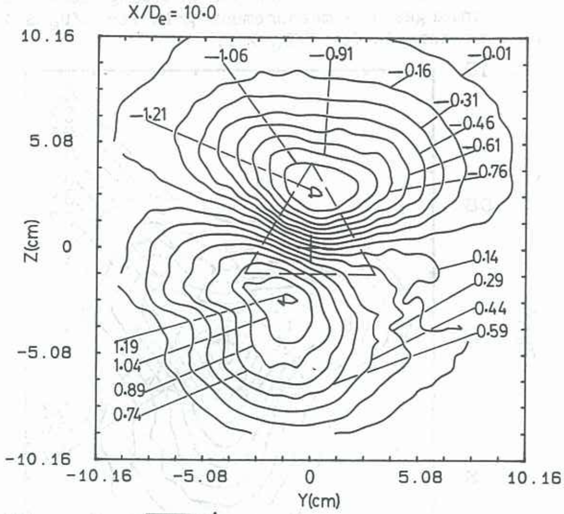


Figure 6b $(\overline{-u'w'}/U^2_{C\ell}$ x 100) contours at $X/D_e$ = 10.0

CONCLUSIONS

The mean flow and turbulence characteristics of an incompressible, isothermal, turbulent free air jet, issuing from a sharp-edged equilateral triangular slot, have been examined in detail. It was found that the jet spreads faster on its base side than on its apex side. The faster base-side spreading leads to an inversion of the jet shape at about five equivalent slot diameters downstream of the slot exit plane. Reynolds shear stress levels in the triangular jet are higher than those found in round turbulent free jets. This is an indication of improved mixing.


ACKNOWLEDGMENTS

The support of the Natural Science and Engineering Research Council of Canada, through grant A5484, is gratefully acknowledged.


REFERENCES


BRADSHAW, P. (1975) An introduction to turbulence and its measurement. Pergamon, Oxford.

BRADSHAW, P. (1987) Turbulent secondary flows. Ann. Rev. Fluid Mech., 19, pp. 53-74.

DAUGHERTY, R.L., FRANZINE, J.B. and FINNEMORE, E.J. (1985) Fluid Mechanics with Engineering Applications. 8th. edition, McGraw-Hill, New York.

GUTMARK, E., SCHADOW, K.C., PARR, D.M., HARRIS, C.K. and WILSON, K.C. (1985) The mean and turbulent structure of noncircular jets. AIAA paper no. 85-0543.

KOSHIGOE, S., GUTMARK, E. and SCHADOW, K.C. (1988) Wave structures in jets of arbitrary shape. III. Triangular jets. Phys. Fluids, 31, pp. 1410-1419.

QUINN, W.R. and MILITZER, J. (1988) Experimental and numerical study of a turbulent free square jet. Phys. Fluids, 31, pp. 1017-1025.

SCHADOW, K.C., GUTMARK, E., PARR, D.M. and WILSON, K.C. (1988) Selective control of flow coherence in triangular jets. Exp. Fluids, 6, pp. 129-135.

WYGNANSKI, I. and FIEDLER, H. (1969) Some measurements in the self-preserving jet. J. Fluid Mech., 38, pp. 577-612.